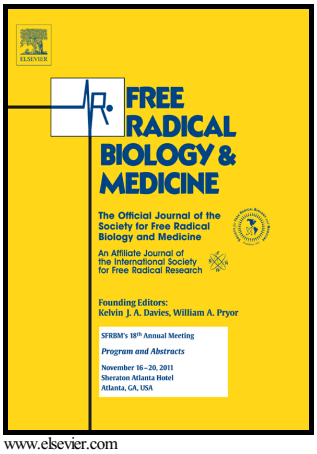

www.elsevier.com

Melatonin receptor activation provides cerebral protection after traumatic brain injury by mitigating oxidative stress and inflammation via the Nrf2 signaling pathway

Junmin Wang, Chao Jiang, Kun Zhang, Xi Lan, Xuemei Chen, Weidong Zang, Zhongyu Wang, Fangxia Guan, Changlian Zhu, Xiuli Yang, Hong Lu, Jian Wang

PII: S0891-5849(18)32261-5
DOI: https://doi.org/10.1016/j.freeradbiomed.2018.12.014
Reference: FRB14074

To appear in: *Free Radical Biology and Medicine*

Received date: 25 October 2018
Revised date: 9 December 2018
Accepted date: 12 December 2018

Cite this article as: Junmin Wang, Chao Jiang, Kun Zhang, Xi Lan, Xuemei Chen, Weidong Zang, Zhongyu Wang, Fangxia Guan, Changlian Zhu, Xiuli Yang, Hong Lu and Jian Wang, Melatonin receptor activation provides cerebral protection after traumatic brain injury by mitigating oxidative stress and inflammation via the Nrf2 signaling pathway, *Free Radical Biology and Medicine,* https://doi.org/10.1016/j.freeradbiomed.2018.12.014

Free Radical Biology and Medicine (FRBM_2018_725R1)

Melatonin receptor activation provides cerebral protection after traumatic brain injury by mitigating oxidative stress and inflammation via the Nrf2 signaling pathway

Junmin Wang[a,b,c,d,1, 2], Chao Jiang[e,1], Kun Zhang[f], Xi Lan[d], Xuemei Chen[b], Weidong Zang[b], Zhongyu Wang[g,d], Fangxia Guan[a,c,f], Changlian Zhu[c,h,i], Xiuli Yang[J], Hong Lu[a,2], Jian Wang[d, 2]

[a]Department of Neurology, The First Affiliated Hospital of Zhengzhou University, Zhengzhou, Henan 450000, China.

[b]Department of Anatomy, College of Basic Medical Sciences, Zhengzhou University, Zhengzhou, Henan 450000, China.

[c]The Third Affiliated Hospital of Zhengzhou University, Zhengzhou, Henan 450052, China.

[d]Department of Anesthesiology and Critical Care Medicine, Johns Hopkins University School of Medicine, Baltimore, MD 21205, USA.

[e]Department of Neurology, The Fifth Affiliated Hospital of Zhengzhou University, Zhengzhou, Henan 450052, China.

[f]School of Life Science, Zhengzhou University, Zhengzhou, Henan 450000, China.

[g]Department of Anesthesiology, The First Affiliated Hospital of Zhengzhou University, Zhengzhou, Henan 450000, China.

[h]Henan Key Laboratory of Child Brain Injury, Institute of Neuroscience, Zhengzhou University, Zhengzhou, Henan 450052, China

[i]Center for Brain Repair and Rehabilitation, Institute of Neuroscience and Physiology, University of Gothenburg, Göteborg 40530, Sweden

[J]Department of Neurosurgery, University of Maryland School of Medicine, Baltimore, MD 21201, USA.

Running title: Ramelteon protects against TBI

[1]These authors contributed equally to this work.

[2]Corresponding authors:

Junmin Wang, Department of Neurology, The First Affiliated Hospital of Zhengzhou University, Zhengzhou, Henan 450000, China

Hong Lu, Department of Neurology, The First Affiliated Hospital of Zhengzhou University, Zhengzhou, Henan 450000, China

Jian Wang, Department of Anesthesiology and Critical Care Medicine, Johns Hopkins University School of Medicine, 720 Rutland Ave, Ross Bldg 370B, Baltimore, MD 21205, USA.

Email addresses: wangjunmin@zzu.edu.cn (Junmin Wang), zzu_luhong@163.com (H. Lu), jwang79@jhmi.edu (Jian Wang)

Abbreviations: ARE, antioxidant response element; ELISA, enzyme-linked immunosorbent assay; FST, forced swim test; GFAP, glial fibrillary acidic protein; GSH, glutathione; GSH-Px, glutathione peroxidase; HO, heme oxygenase; Iba-1, ionized calcium-binding adapter; KO, knockout; MWM, Morris water maze; NOR, novel object recognition; Nrf2, NF-E2-related factor; mNSS, modified neurological severity score; SOD, superoxide dismutase; SPT, sucrose preference test; TBI, traumatic brain injury; TST, tail suspension test.

Abstract

Traumatic brain injury (TBI) is a principal cause of death and disability worldwide. Melatonin, a hormone made by the pineal gland, is known to have anti-inflammatory and antioxidant properties. In this study, using a weight-drop model of TBI, we investigated the protective effects of ramelteon, a melatonin MT1/MT2 receptor agonist, and its underlying mechanisms of action. Administration of ramelteon (10 mg/kg) daily at 10:00 am alleviated TBI-induced early brain damage on day 3 and long-term neurobehavioral deficits on day 28 in C57BL/6 mice. Ramelteon also increased the protein levels of interleukin (IL)-10, IL-4, superoxide dismutase (SOD), glutathione, and glutathione peroxidase and reduced the protein levels of IL-1β, tumor necrosis factor, and malondialdehyde in brain tissue and serum on days 1, 3, and 7 post-TBI. Similarly, ramelteon attenuated microglial and astrocyte activation in the perilesional cortex on day 3. Furthermore, ramelteon decreased Keap 1 expression, promoted nuclear factor erythroid 2-related factor 2 (Nrf2) nuclear accumulation, and increased levels of downstream proteins, including SOD-1, heme oxygenase-1, and NQO1 on day 3 post-TBI. However, in Nrf2 knockout mice with TBI, ramelteon did not decrease the lesion volume, neuronal degeneration, or myelin loss on day 3; nor did it mitigate depression-like behavior or most motor behavior deficits on day 28. Thus, timed ramelteon treatment appears to prevent inflammation and oxidative stress via the Nrf2-antioxidant response element pathway and might represent a potential chronotherapeutic strategy for treating TBI.

Graphical abstract

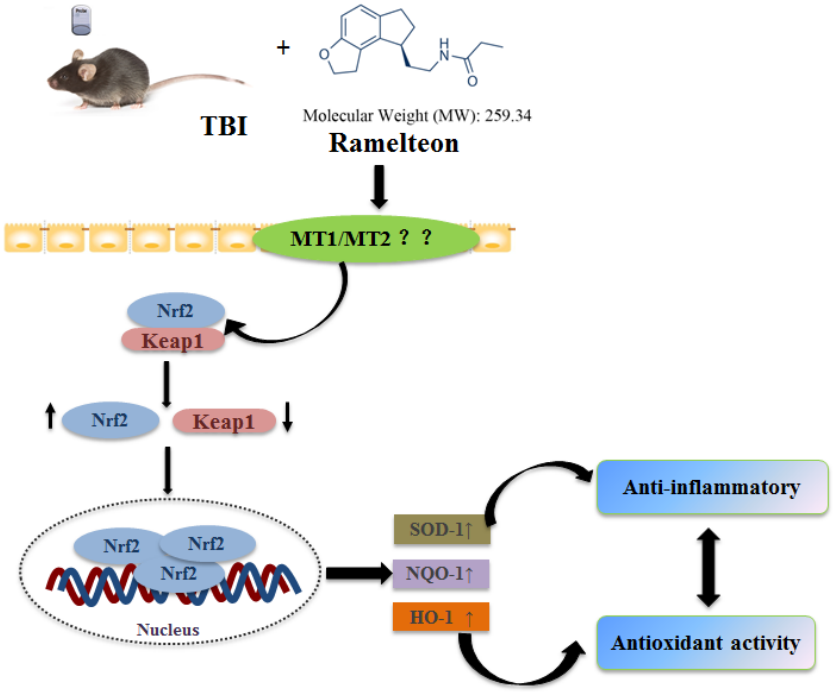

Keywords: Chronotherapy; Inflammation; NF-E2-related factor; Oxidative stress; Ramelteon; Traumatic brain injury

1. Introduction

Traumatic brain injury (TBI) is estimated to affect over 10 million people annually and represents the leading cause of disability and death among those under 45 years old [1]. In the United States, the occurrence of TBI is increasing, with more than 1.7 million cases each year [2]. The pathophysiology of TBI involves two typical processes: primary injury, which is initiated directly by the trauma, and secondary injury, which is caused by inflammation, oxidative stress, and glutamate excitotoxicity. These secondary processes lead to additional

brain injury, including edema and cell death.

Melatonin [N-acetyl 5-methoxytryptamine, MT; Supplementary Fig. 1] is a hormone made by the pineal gland that exhibits non-enzymatic, antioxidant, and neuroprotective effects in various models of brain injury, including TBI [3]. The physiologic effect of melatonin is mediated by its three membrane receptors (MT1, MT2, and MT3) [4]. MT1 and MT2 have been localized to discrete brain areas of the rodent nervous system, including the suprachiasmatic nucleus (SCN), cerebellum, thalamus, hippocampus, and peripheral tissues [5], whereas MT3, now defined as quinone reductase II, is highly expressed in the liver and the kidneys, with moderate amounts in the heart, adipose tissue, and brain [6]. Melatonin enhances immune function, has anti-inflammatory properties [7], regulates radical scavengers [8], and modulates mood and behavior [9] by activating the MT1 and/or MT2 receptors located mainly in the SCN of the hypothalamus [5]. Importantly, it can decrease brain edema, attenuate blood-brain barrier permeability, and diminish cortical astrocyte activation and neuronal death in animal models of TBI, likely by inhibiting oxidative stress [10-12]. In addition, it has been shown to attenuate TBI-induced inflammatory response and ameliorate behavioral deficits [13].

Ramelteon [(S)-N-[2-(1,6,7,8-tetrahydro-2H-indeno-[5,4-b]furan-8-yl)ethyl] propionamide; TAK-375; Supplementary Fig. 1] is a selective melatonin MT1/MT2 receptor agonist with a molecular weight of 259.34. It was approved by the Food and Drug Administration for treating insomnia in 2005 [4, 14]. It is remarkably free of side effects, in part because of its high affinity for MT1 and MT2 receptors and negligible affinity for MT3 or other receptors. Its affinity for MT1 and MT2 receptors is 3-16 times that of melatonin [5],

and after oral administration, it is absorbed rapidly (0.5-1.5 h) and has a half-life (1.0-2.6 h) longer than that of melatonin (<30 min) [15, 16]. Ramelteon has been shown to penetrate the brain [17] and exert neuroprotection [18].

Ramelteon has been used to treat sleep disturbance in patients with TBI [19], but its neuroprotective effects have not been investigated in patients or in animal models of TBI. It is unknown whether timed ramelteon treatment can mitigate oxidant stress and brain inflammatory response after TBI. Therefore, in this study, using Feeney's weight-drop model of TBI in mice [20], we assessed whether timed ramelteon treatment provides neuroprotective, antioxidative, or anti-inflammatory effects and investigated its potential mechanisms of action.

2. Materials and methods

2.1 Mice

Male C57BL/6 wild-type mice (20-25 g, 3 months old) were purchased from the Laboratory Animal Center of Zhengzhou University (Henan province, China), and male Nrf2 gene knockout (KO) mice (C57BL/6 background, 20-25 g, 3 months old) were originally generated by Dr. Masayuki Yamamoto [21]. Animals were housed in a pathogen-free animal facility with a 12-h light/dark cycle (lights on from 8:00 am to 8:00 pm), food and water available ad libitum, a room temperature of 24±1°C, and humidity of 60±10% for at least 1 week before the experiment. The experimental procedures were approved by the Animal Care and Use Committees of Zhengzhou University. Animal experiments are reported in accordance with the ARRIVE guidelines.

2.2 Feeney's weight-drop model of TBI

We used Feeney's weight-drop model of TBI to produce a contusion injury of the right parietal cortex in mice, as we described previously [22, 23]. The mice were anesthetized with an intraperitoneal injection of 10% chloral hydrate (0.035 mL/10 g), and the head was fixed in a stereotactic device. Under aseptic conditions, a midline longitudinal incision was made over the skull, and a 4-mm craniotomy was made with a dental drill and trephine over the right parietal bone window 1 mm behind the bregma and 1 mm to the midline. A 20-g steel rod with a flat end (3 mm in diameter) was released from a height of 20 cm onto a piston resting on the dura to a controlled depth of 1 mm. The scalp was then closed with cyanoacrylate tissue glue. After this procedure, the mice were returned to their home cages and maintained at room temperature (24 ± 1°C). The sham control group underwent surgical incision but did not receive the cortical impact.

2.3 Experimental groups and drug administration

Ramelteon (purity=99.63%, Selleck Chemicals, Houston, TX) was suspended in 0.5% methylcellulose solution as described previously [24]. Mice were assigned randomly (http://www.randomization.com) [21, 25] to receive ramelteon (10 mg/kg) or vehicle (0.5% methylcellulose, Sigma, Shanghai, China) by gavage at 1 h after TBI and then once daily at approximately 10:00 am for 28 days. This chronotherapeutic strategy was based on the low pineal and blood levels of melatonin in mice at around 10:00 am [26, 27]. We chose the delivery route, drug dosing, drug preparation, and treatment regimen for ramelteon based on

prior studies [24, 28, 29].

A total of 170 wild-type mice and 64 Nrf2 KO mice were included in this study. Animals that died before the end of the study (n = 16) were excluded from the final data analysis. Brain water content and lesion volume were measured in eight to 10 mice per group. We used five to 10 mice per group to assess behavioral performance, measure lesion volume by histology, and determine changes in protein expression by ELISA and Western blot. Treatment, data collection, and data analyses were blinded by using different investigators or by masking sample labels with coded numbers. Supplementary Fig. 2 summarizes the experimental timeline.

2.4 Neurologic function testing

The modified neurologic severity score (mNSS) test was used to measure neurologic function on days 1, 3, 7, 14, 21, and 28 after TBI based on our previous studies [30-32]. The mNSS consists of motor (muscle status and abnormal movement), sensory (visual, tactile, and proprioceptive), reflex, and balance tests, and is graded on a scale of 0 (normal) to 18 (maximal deficit).

2.5 Measurement of cerebral edema

Brain water content was measured by the wet-dry weight ratio method as described previously [33, 34]. It was calculated as a percent using the following equation: brain water content (%) = (wet weight – dry weight)/wet weight ×100% [35].

2.6 Forced swim test (FST)

During the FST, mice were placed individually in a clear Perspex cylinder (65 cm high × 25 cm in diameter) filled to a depth of 15 cm with tap water at 25 ± 1°C. The movements of the mice on day 28 after TBI were recorded by a camera for 6 min, and the duration of immobility was recorded during the last 4 min of the test by an investigator blinded to the experimental groups. The absence of escape-oriented behaviors such as swimming, jumping, rearing, sniffing, or diving is indicative of behavioral despair. ANYMaze software was used to track and analyze the data. Mice that were floating upright and making only small movements to remain above water were considered immobile [36-38].

2.7 Tail suspension test (TST)

The TST was performed on 28 day after TBI according to our established protocol [37-39]. Mice were acclimated to the behavior room for 1 h and then suspended by their tails to the edge of a shelf 55 cm above a desk. The tail was attached to the shelf with adhesive tape (17 cm long, positioned approximately 1 cm from the tip of the tail). A plastic tube (4 cm long, 1 cm diameter, 1.5 g) placed around the tail prevented the mouse from climbing its tail. Behaviors were recorded with a video camera for 6 min. The immobility time was calculated by subtracting the total amount of mobility time from the 360 s of test time. Mice were considered immobile only when they hung passively and completely motionless.

2.8 Sucrose preference test (SPT)

The SPT was performed as described previously on day 21 post-TBI [21, 37, 38]. Mice

were trained with two identical bottles containing 1% sucrose solution (w/v) for 3 days, followed by one bottle of 1% sucrose solution and one bottle of plain tap water for 4 days. The respective weights of the sucrose solution and water consumed before and after the test were measured. Sucrose preference was calculated with the following equation: % sucrose preference = sucrose intake in g / (sucrose solution intake + tap water intake in g) × 100% [21].

2.9 Morris water maze test (MWM)

We tested mice in the MWM test to evaluate spatial memory on days 23-28 after TBI according to the protocols reported previously [36, 40, 41]. Animals were trained to find a hidden platform in a circular aluminum pool (180 cm in diameter and 50 cm deep) that was surrounded by visual cues placed at the same starting point over 5 consecutive training days before the test. The test (probe trial) was performed on the last day. Trajectory and navigation parameters were recorded and analyzed by ANYMaze video tracking system (Version 4.8; Stoelting Co., Wood Dale, IL).

2.10 Novel object recognition (NOR) test

The NOR test was used to evaluate recognition memory on day 28 after TBI as described previously [21, 22, 38]. The discrimination index was used to assess cognitive ability and was calculated as follows: Discrimination index (%) = time spent with novel object/(time spent with novel object + time spent with old object) × 100% [37].

2.11 Wire hanging test

The wire-hanging test was performed on days 7, 14, and 28 after TBI. It was carried out as described previously with minor modification to evaluate limb muscle strength, balance, and endurance [21, 37]. The mice were placed on a 55-cm long horizontal metallic wire (1 mm in diameter) that was stretched between two posts, 50 cm above a soft pillow. The latency to fall was recorded up to 600 s. Hind limbs of the mice were gently covered with adhesive tape to prevent them from using all four paws.

2.12 Forelimb placement test

Mice were trained in the forelimb placement test before TBI and then tested at 7, 14, and 28 days after TBI [21, 42]. We gently held the mouse by the torso and brushed its vibrissae against the edge of a tabletop. Placing was calculated as the percentage of successful reaches in 10 trials.

2.13 Rotarod test

On days 7, 14, and 28 after TBI, we tested mice on an accelerating rotarod apparatus to measure motor function and balance [21, 43, 44]. Each mouse was placed in a neutral position on the rod (4 cm in diameter). The rod then began to rotate with accelerating speed (1 rpm/5 s) linearly from 1 rpm. An arbitrary time limit of 5 min was set on the apparatus during the training (3 adaptation trials) and testing procedures. The time spent on the rotarod was recorded as latency to fall.

2.14 Tissue processing for histology

On day 3 after TBI, six mice in each group were anesthetized with an overdose of 10% chloral hydrate and transcardially perfused via the left ventricle with 0.1 M phosphate-buffered saline (PBS, pH 7.4) followed by 30 mL of 4% paraformaldehyde. The brains were removed, postfixed in 4% paraformaldehyde overnight at 4°C, and then transferred sequentially into 15%, 25%, and 35% sucrose solution overnight prior to dissection and sectioning [45]. The brain tissue was embedded in Tissue-Tek® O.C.T. compound (Sakura Finetek Inc, Torrance, CA) and serially sectioned into 25 μm coronal sections on a cryostat (Leica, Germany). Sections were then collected into six-well plates containing PBS for histology.

2.15 Determination of lesion volume and neuronal death

On day 3 after TBI, coronal brain sections from C57BL/6 mice treated with ramelteon or vehicle were stained with Cresyl violet (for Nissl bodies) and mounted with DPX mounting medium. Sixteen sections from every six brain sections throughout the whole hemisphere were selected from each mouse for measurement of lesion volume. Similarly, the brain sections from Nrf2 KO mice treated with ramelteon or vehicle were stained with Cresyl violet and Luxol Fast Blue (for myelin) or Fluoro-Jade C (FJC, for degenerating neurons), as previously reported [21]. Image J software (NIH, Bethesda, MD, USA) was used to quantify lesion volume, myelin loss, and degenerating neurons in the striatum. The volume of the lesion in cubic millimeters was calculated as the sum of the damaged areas of each section multiplied by the interslice distance. The presence of normal myelin was expressed as a

percentage of the total area examined. The degenerating neurons were counted in three fields immediately adjacent to the injured area at a magnification of 200× over a microscopic field of 0.1 mm^2 and expressed as cells per square millimeter [46].

2.16 Immunofluorescence staining of GFAP and Iba-1

We performed immunofluorescence staining of the coronal brain sections to examine the activation of astrocytes [glial fibrillary acidic protein (GFAP)-positive] and microglia [ionized calcium-binding adaptor molecule 1 (Iba-1)-positive] as described previously [46-48]. After being blocked for 1 h, the sections were incubated with rabbit anti-GFAP (1:500, Proteintech, Rosemont, IL) or rabbit anti-Iba-1 (1:300, Proteintech) overnight at 4°C and then with secondary antibody (CY3-conjugated donkey anti-rabbit lgG, Sangon Biotech, Songjiang, Shanghai) for 1 h at room temperature. Nuclei were labeled with 4,6-diamidino-2-phenylindole (DAPI; D8417; 1:1000, Sigma, St. Louis, MO) for 1 min. Fluorescence images were taken with a fluorescence microscope (Olympus, Tokyo, Japan).

2.17 Measurement of cytokines by enzyme-linked immunosorbent assay (ELISA)

At days 1, 3, and 7 after TBI, we measured the levels of cytokines interleukin (IL)-4, IL-10, IL-1β, and TNF-α in blood serum, and oxidative stress biomarkers superoxide dismutase (SOD), malondialdehyde (MDA), glutathione (GSH), and glutathione peroxidase (GSH-Px) in blood serum and brain tissue using ELISA kits (Biotechnology Co., Ltd from Donghu New & High Technology Development Zone, Wuhan and Tsz Biosciences from San Francisco, CA) [34, 49].

2.18 Western blotting

On day 3 after TBI, mice were decapitated under deep anesthesia. Fifty milligrams of brain tissue collected from around the injured area was homogenized in ice-cold lysis buffer supplemented with protease and phosphatase inhibitors. Cytosolic and nuclear protein fractions were isolated with the Nuclear Extraction Kit (Origene, Rockville, MD). Total protein was quantified with the BCA assay (Bio-Rad, Hercules, CA). Western blotting was performed as previously described [21, 25]. The extracted protein was separated by 4-20% sodium dodecyl sulfate-polyacrylamide gel electrophoresis and transferred onto a polyvinylidene difluoride membrane. Membranes were blocked with 5% non-fat milk and incubated with the following primary antibodies: rabbit anti-Nrf2 (1:2000, Abcam, Cambridge, MA), mouse anti-Keap1 (1:1000, Santa Cruz, Dallas, TX), rabbit anti-heme oxygenase (HO)-1 (1:1500, Abcam), mouse anti-NQO1 (1:1000, Novus, Littleton, CO), anti-SOD1 (1:1000, Abcam), mouse anti-β-actin (1:3000, Santa Cruz), and mouse anti-Lamin B (1:1000, Santa Cruz) at 4°C overnight. Then the membranes were incubated with horseradish peroxidase-conjugated anti-mouse or anti-rabbit secondary antibodies (1:3000, Santa Cruz) and visualized by enhanced chemiluminescence (ECL) solution (Millipore). Images of blots were captured with an ImageQuant ECL Imager (GE Healthcare, Chicago, IL), and the bands were quantified with Image J software.

2.19 Statistical analyses

All statistical analyses were carried out with SPSS Statistical Software (version 21).

Data are presented as mean ± SD with $p<0.05$ being considered statistically significant. Differences between two groups were assessed by unpaired, two-tailed *t*-test. We used a one-way or two-way ANOVA and Bonferroni post hoc test to compare differences among multiple groups.

3. Results

3.1 Ramelteon reduced brain lesion volume and edema after TBI

Cresyl violet staining showed that lesion volumes were significantly smaller in the ramelteon group than in the vehicle group on days 3 (5.66 ± 0.99 mm^3 vs. 7.29 ± 0.82 mm^3) and 28 (8.40 ± 1.14 mm^3 vs. 10.57 ± 1.30 mm^3) after TBI (n = 8 mice/group, $p<0.05$; Figs. 1A, B). In addition, brain edema, as measured by brain water content of the ipsilateral hemisphere, was significantly lower in the ramelteon group than in the vehicle group on day 3 after TBI (77.90 ± 1.92% vs. 81.77 ± 1.89%; $p<0.05$; n = 10 mice/group; Fig. 1C).

3.2 Ramelteon increased body weight but failed to reduce mortality after TBI

Mice lose body weight in the first week after TBI, but those treated with ramelteon regained weight more quickly than mice treated with vehicle (Day 7: $p<0.05$, n=10 mice/group; Fig. 1D). Nevertheless, ramelteon failed to reduce mortality on day 7 after TBI ($p>0.05$, n=10 mice/group; Fig. 1E).

3.3 Ramelteon ameliorated neurologic deficits and depression-like behavior after TBI

The mNSS increased markedly in the first day after TBI and then gradually decreased in

all groups with time. Beginning after the first day, the scores in the ramelteon-treated TBI group remained significantly lower than those in the vehicle-treated TBI group for 4 weeks (p<0.05, n=10 mice/group; Fig. 1F). In both the FST and TST, the immobility time in the ramelteon-treated TBI group was significantly lower than that of the vehicle-treated TBI group (86.83 ± 16.15 s vs. 109.60 ± 21.53 s in the FST; 101.70 ± 20.61 s vs. 135.90 ± 19.13 s in the TST) on day 28 (F = 5.880, 13.27, respectively; both p<0.05, n = 10 mice/group; Figs. 1G and H). Furthermore, the ramelteon-treated TBI mice consumed more sucrose-sweetened water (62.85 ± 12.51%) than the vehicle-treated TBI mice did (47.05 ± 10.96%) in the sucrose preference test (F = 6.411, p<0.05, n = 10 mice/group; Fig. 1I), though the total liquid consumed did not differ between the two groups (Supplementary Fig. 3).

3.4 Ramelteon improved cognitive deficits after TBI

The MWM and NOR test were used to evaluate cognitive impairment after TBI. In the MWM test, mice that find the platform more quickly are interpreted as having better learning and memory function. Performance during training on days 23 to 27 and during the probe trial on day 28 was evaluated by analyzing the percentage of time spent swimming toward the platform. The ramelteon-treated TBI mice spent significantly more time in the target quadrant trajectory than did the vehicle-treated TBI mice across the training days and the probe trial period (Fig. 2A). The ramelteon-treated TBI mice exhibited significantly shorter escape latency than did the vehicle-treated TBI mice on the last two days of training (day 26: 21.5 ± 2.9 s vs. 27.6 ± 3.9 s; day 27: 19.7 ± 1.6 s vs. 27.7 ± 2.4 s; both p<0.05, n=10 mice/group; Fig. 2B). However, the average swimming speed did not differ among the ramelteon-treated,

vehicle-treated, and sham groups during the training days (Fig. 2C) or the probe trial (Fig. 2D) ($F = 0.9342$, both $p>0.05$, n = 10 mice/group), suggesting that ramelteon did not alter the swimming ability. The ramelteon-treated TBI mice also had significantly greater retention time in the target quadrant (29.3 ± 4.8 s) and more platform crossings (3.7 ± 1.2 times) than did vehicle-treated TBI mice (20.5 ± 5.7 s, 2.1 ± 1.0 times) during the probe trial ($F = 16.78$, 11.24, respectively, both $p<0.05$, n = 10 mice/group; Figs. 2E and F). Moreover, TBI caused a clear decrease in the discrimination index of the NOR test (49.72 ± 9.6% vs. 74.19 ± 11.5%) that was reversed by ramelteon administration (62.60 ± 11.5% vs. 49.72 ± 9.6%, $F = 12.66$, both $p<0.05$, n = 10 mice/group; Fig. 2G).

3.5 Ramelteon increased anti-inflammatory cytokines and reduced pro-inflammatory cytokines after TBI

TBI is associated with altered cytokine profiles in the blood and brain tissue. To investigate the role of inflammatory response after TBI, we determined serum and brain levels of IL-10, IL-4, IL-1β, and TNF-α on days 1, 3, and 7 after TBI. TBI induced secretion of pro-inflammatory cytokines IL-1β and TNF-α and anti-inflammatory cytokines IL-10 and IL-4 in the brain tissue and serum of vehicle-treated mice during the experimental period (Fig. 3A and B). Brain and serum levels of these four cytokines increased over time after TBI induction. Compared with vehicle treatment, ramelteon treatment significantly increased brain and serum IL-10 and brain IL-4 on days 1, 3, and 7, as well as serum IL-4 on day 7. In contrast, ramelteon significantly decreased brain IL-1β on days 3 and 7; serum IL-1β on day 7; brain TNF-α on days 1, 3, and 7; and serum TNF-α on days 3 and 7 compared with levels

in vehicle-treated mice (all $p<0.05$, n = 6 mice per group).

3.6 Ramelteon attenuated oxidative stress after TBI

We measured SOD, MDA, GSH, and GSH-Px levels in brain tissue and serum on days 1, 3, and 7 after TBI to determine whether ramelteon attenuated oxidative damage in the central and peripheral systems. SOD, GSH, and GSH-Px levels were decreased in brain tissue and serum after TBI, whereas MDA was increased, when compared with levels in the sham group on days 1, 3, and 7 ($p<0.05$, n = 6 mice/group). Ramelteon reversed these changes. Ramelteon-treated mice displayed significantly higher brain concentrations of SOD and GSH on days 1, 3, and 7, and higher GSH-Px on days 1 and 7, than did vehicle-treated mice ($p<0.05$, n = 6 mice/group). Ramelteon also significantly increased the serum levels of SOD and GSH-Px at all three time points and GSH on days 1 and 3 compared with those in the vehicle group ($p<0.05$, n = 6 mice/group). Moreover, ramelteon-treated mice had significantly lower levels of brain and serum MDA on days 1, 3, and 7 than did vehicle-treated mice (all $p<0.05$, n = 6 mice/group). Overall, ramelteon treatment increased brain and serum levels of SOD, GSH, and GSH-Px and decreased serum levels of MDA at most of the three time points tested (Fig. 3B).

3.7 Ramelteon inhibited activation of astrocytes and microglia in the perilesional cortex after TBI

We assessed microglia/macrophage and astrocyte activation with Iba-1 and GFAP immunofluorescence labeling, respectively. Microglial/macrophage activation was classified

by morphologic criteria and a cell body diameter cutoff of 7.5 mm [45, 50]. In mice with TBI, the immunoreactivity of reactive astrocytes was more intense and the processes were longer and thicker, as we have previously described [51]. Immunofluorescence staining of GFAP and Iba-1 on day 3 showed that astrocytes and microglia were activated in the perilesional area of the injured cortex. However, this activation was markedly decreased in the ramelteon-treated TBI group ($F = 39.58, 32.02$, $p<0.05$, n = 6 mice/group). Furthermore, the branches of the astrocytes tended to be larger in the vehicle-treated TBI group than in the sham group (Fig. 3C). Microglia from the vehicle-treated TBI mice had enlarged, round cell bodies and shortened processes, whereas those from the ramelteon-treated TBI mice exhibited a less activated phenotype with smaller cell bodies and elongated processes (Fig. 3D). The numbers of activated astrocytes and microglia surrounding the lesion were determined by counting cells in four sites within a specified sampling zone selected from the ipsilateral dorsal parietal cortex (Supplementary Fig. 4).

3.8 Ramelteon decreased Keap1 expression, promoted Nrf2 nuclear accumulation, and increased SOD1, HO-1, and NQO1 expression after TBI

Nrf2 is a key transcription factor that regulates antioxidant enzymes [21, 52]. Under conditions of oxidative stress, it is released from the Keap1-Nrf2 complex in the cytoplasm, and its free form translocates to the nucleus. Therefore, we measured cytoplasmic Keap1 protein expression and cytoplasmic and nuclear Nrf2 protein expression on day 3 after TBI. Ramelteon significantly reduced cytosolic Keap1 expression compared with that in the vehicle-treated TBI group ($F = 21.91$, $p<0.05$, n = 5 mice/group; Fig. 4A) and increased

nuclear Nrf2 expression (F = 58.31, $p<0.05$, n = 5 mice/group; Fig. 4B) without altering cytoplasmic Nrf2 expression (F = 0.5776, $p>0.05$, n = 5 mice/group; Fig. 4C). Furthermore, expression levels of Nrf2 downstream molecules SOD1, HO-1, and NQO1 were increased after TBI compared with those in the sham group and were further increased by ramelteon (F = 16.86, 20.26, 18.93, respectively, all $p<0.05$, n = 5 mice/group; Fig. 4D-F).

3.9 Neuroprotection by ramelteon was mostly lost in Nrf2 KO mice

To assess whether ramelteon protects against TBI via the Nrf2-antioxidant response element (ARE) signaling pathway, we administered ramelteon to Nrf2 KO mice subjected to TBI. Lesion volume on day 3 and survival rate during the first 7 days after TBI did not differ between the vehicle- and ramelteon-treated Nrf2 KO mice (both $p>0.05$, n = 10 mice/group; Fig. 5A-C). In contrast, ramelteon significantly increased body weight of TBI mice on day 3 ($p<0.05$, n = 10 mice/group; Fig. 5D) and decreased the neurologic deficit scores compared with those of the vehicle group on days 14 and 28 (both $p<0.05$, n = 10 mice/group; Fig. 5E). However, ramelteon failed to improve performance of Nrf2 KO mice in the wire hanging test, rotarod test, and forelimb placement test on days 7, 14, and 28 (all $p>0.05$, n = 10 mice/group; Fig. 5F-H). Furthermore, ramelteon treatment did not improve performance of Nrf2 KO mice in the NOR test (Fig. 5I), TST (Fig. 5J), FST (Fig. 5K), or SPT (Fig. 5L and Supplementary Fig. 3B) compared with that of vehicle-treated mice on day 28 after TBI (F = 11.14, 19.07, 5.918, 6.950, and 0.7026, respectively, all $p>0.05$, n = 10 mice/group). Additionally, ramelteon failed to increase the percentage of area with normal myelin, as assessed by Luxol fast blue staining (F = 8.695, $p>0.05$, n = 6 mice/group; Fig. 5M and Supplementary Fig. 4C),

or decrease the number of degenerating neurons, as measured by Fluoro-Jade C staining, in the perilesional area of the Nrf2 KO mice on day 3 ($F = 359.8$, $p>0.05$, n = 6 mice/group; Fig. 5N).

4. Discussion

Using young adult mice subjected to a weight-drop model of TBI, we evaluated the protective effects of ramelteon and elucidated its potential mechanism of action. We found that ramelteon reduced brain lesion volume on days 3 and 28, reduced brain edema on day 3, and improved neurologic function on day 28 after TBI. In addition, ramelteon ameliorated depression-like behavior and cognitive deficits, and attenuated the TBI-induced pro-inflammatory response and oxidative stress. Importantly, it reduced Keap1 expression, promoted Nrf2 nuclear accumulation, and increased the expression of Nrf2 downstream molecules SOD1, HO-1, and NQO1. However, in Nrf2 KO mice, ramelteon failed to 1) decrease lesion volume, neuronal death, and myelin loss; 2) mitigate the motor deficits in the wire-hanging test, rotarod test, and forelimb placement test; and 3) ameliorate the cognitive deficits and depression-like behaviors. However, ramelteon did modestly decrease neurologic deficit score after TBI in Nrf2 KO mice. Together, these novel findings provide evidence that ramelteon attenuates TBI-induced brain damage primarily through the Nrf2-ARE signaling pathway.

TBI can cause damage to the cingulate, a part of the brain situated in the medial aspect of the cerebral cortex that has been shown to affect a variety of neurobehavioral functions, including cognition and emotion [53]. In addition to motor deficits, our TBI mice

exhibited cognitive deficits and depression-like behavioral abnormalities, which were mitigated by long-term ramelteon treatment, suggesting that prolonged melatonin receptor activation might be able to help repair brain tissue and promote functional recovery.

Inflammation is one of the major determinants of secondary brain damage after TBI [54]. Melatonin was reported to restrain microglial and astrocyte activity and alleviate neuroinflammation in animal models of TBI [10, 55]. Although ramelteon inhibits the systemic inflammatory response in patients with insomnia, probably via the MT receptors [56], it is unclear whether it inhibits inflammatory response in the TBI model. In this study, we provide evidence that ramelteon markedly increases the protein level of anti-inflammatory cytokines (IL-4 and IL-10) while decreasing the level of pro-inflammatory cytokines (IL-1β and TNF-α) in brain tissue and serum on days 1, 3, and 7 post-TBI. Moreover, ramelteon decreased TBI-induced microglial and astrocyte activation as shown by decreased Iba-1 and GFAP immunoreactivity, supporting the notion that ramelteon has anti-inflammatory effects after TBI.

The neuroprotective effects of melatonin might also be attributed to its ability to induce antioxidant enzymes. This property might be correlated with the activation of MT1 and/or MT2 melatonin receptors [1]. In this study, we assessed the brain's antioxidant status by measuring four major oxidative stress biomarkers. We found that ramelteon significantly increased brain and serum levels of SOD, GSH, and GSH-Px on days 1, 3, and 7 post-TBI while levels of MDA were correspondingly reduced. These effects might be due to ramelteon's ability to activate the ARE, which regulates key cellular antioxidants. A prior study showed that ramelteon reduced protein oxidation in the hippocampus of transgenic

mice in a model of Alzheimer's disease [57]. Because melatonin has anti-inflammatory and antioxidative properties, its low levels in pineal gland and blood of mice at around 10:00 am [26, 27] may indicate that the inflammatory response and oxidative stress are highest at that time. The efficacy of our treatment regimen supports a timed drug administration strategy (chronopharmacology) to combat proinflammatory response and oxidative stress after TBI.

The molecular mechanisms of action of ramelteon after TBI are unknown, but the Nrf2-ARE pathway could be involved. The transcription factor Nrf2 plays an indispensable role in the induction of endogenous antioxidant enzymes [52, 58]. The Nrf2-ARE system is considered to be a multi-organ protector and is fundamentally neuroprotective in several brain diseases, including TBI [21, 52, 58-60] and intracerebral hemorrhage [52, 61]. Under physiologic conditions, Nrf2 binds with its negative regulator, Keap1, in the cytoplasm; however, under conditions of oxidative stress or injury, Nrf2 is liberated from the Keap1-Nrf2 complex and translocates into the nucleus, where it activates the Nrf2-ARE pathway [21]. Therefore, we investigated changes in the Nrf2-ARE signaling pathway after ramelteon administration. We found that ramelteon reduced levels of MDA and Keap1 in the brains of mice with TBI. Moreover, ramelteon increased nuclear accumulation of Nrf2 and cytoplasmic expression of phase II enzymes SOD1, HO-1, and NQO1, which can decrease oxidative stress. Thus, ramelteon might increase Nrf2 expression at its post-translational level after TBI. These results reveal that the Nrf2-ARE signaling pathway was enhanced by ramelteon treatment.

Evidence supports a critical role for Nrf2 in counteracting the inflammatory response in TBI models [59]. It has been reported that, when subjected to a TBI model, Nrf2 KO mice

produce greater levels of TNF-α, IL-1β, and IL-6 than do wild-type mice [62]. Our data indicate that ramelteon differentially regulates anti- and pro-inflammatory cytokine production via the Nrf2-ARE pathway. After TBI, Nrf2 is highly induced in neurons, astrocytes, and microglia [63-66]. In a recent study, Dong *et al*. reported that Nrf2 immunoreactivity was co-localized predominantly with NeuN-positive cells, but this accumulation was transient, as fewer neurons ($NeuN^+$) were Nrf2-positive at 3 days post-TBI. In contrast, Nrf2 expression was continuously high in microglia, particularly at 3 and 7 days post-injury. The ratio of Nrf2-positive cells in $Iba1^+$ cells peaked at 7 days. In addition, slight, but stable Nrf2 immunoreactivity was detected in astrocytes ($GFAP^+$) from 6 h to 21 days after TBI. Most $GFAP^+$ cells co-stained for Nrf2 at 7 days post-TBI, and Keap 1 exhibited the same expression pattern as Nrf2 [67].

To confirm that ramelteon protects against TBI via the Nrf2-ARE signaling pathway, we treated Nrf2 KO with ramelteon after TBI and investigated histologic and behavioral outcomes. We found that ramelteon did not decrease lesion volume, neuronal death, or myelin loss or improve performance in most of the behavioral tests (cognition and depression-like behaviors), but it did modestly decrease the neurologic severity score. These results indicate that ramelteon produces cerebroprotection predominantly via the Nrf2-ARE pathway, although its protection might not be solely dependent on this pathway. As indirect evidence, a recent study showed that the neuroprotection conferred by melatonin after TBI was lost in Nrf2 KO mice [60].

Because TBI is most common in young male adults, we chose 3-month-old male mice as the test subjects. We will carry out future studies in female mice to make these preclinical

studies more translatable to the clinic. Interestingly, it was reported that the sex does not influence the effect of ramelteon in humans [68]. Importantly, our data indicate that ramelteon has antioxidant and anti-inflammatory effects; however, we still must determine whether these effects are mediated by MT1, MT2, or both receptors.

In conclusion, we provide the first evidence that ramelteon has antioxidative and anti-inflammatory properties and protects the brain after TBI primarily by targeting the Nrf2-ARE signaling pathway. These findings imply that ramelteon may hold promise for treating TBI and other acute brain insults. A major challenge in the future will be to understand the effects of timed ramelteon treatment on microglial phenotype and cell death pathways and the underlying circadian mechanisms. The insights gained from this study will prompt new chronotherapeutic strategies for treating TBI.

Acknowledgments

The authors thank the Wang lab members for technical expertise and insightful input. This research was supported by a grant from the National Natural Science Foundation of China (Grant No. 81671165 to CJ).

Conflict of interest statement

The authors have disclosed that they do not have any conflicts of interest.

References

[1] Fernandez-Gajardo, R.; Matamala, J. M.; Carrasco, R.; Gutierrez, R.; Melo, R.; Rodrigo, R. Novel therapeutic strategies for traumatic brain injury: acute antioxidant reinforcement. *CNS Drugs* **28:**229-248; 2014.

[2] Zhang, H.; Wang, W.; Jiang, S.; Zhang, Y.; Heo, H. Y.; Wang, X.; Peng, Y.; Wang, J.; Zhou, J. Amide proton transfer-weighted MRI detection of traumatic brain injury in rats. *J Cereb Blood Flow Metab* **37:**3422-3432; 2017.

[3] Yuruker, V.; Naziroglu, M.; Senol, N. Reduction in traumatic brain injury-induced oxidative stress, apoptosis, and calcium entry in rat hippocampus by melatonin: Possible involvement of TRPM2 channels. *Metab Brain Dis* **30:**223-231; 2015.

[4] Emet, M.; Ozcan, H.; Ozel, L.; Yayla, M.; Halici, Z.; Hacimuftuoglu, A. A review of melatonin, its receptors and drugs. *Eurasian J Med* **48:**135-141; 2016.

[5] Liu, J.; Clough, S. J.; Hutchinson, A. J.; Adamah-Biassi, E. B.; Popovska-Gorevski, M.; Dubocovich, M. L. MT1 and MT2 melatonin receptors: a therapeutic perspective. *Annu Rev Pharmacol Toxicol* **56:**361-383; 2016.

[6] Slominski, R. M.; Reiter, R. J.; Schlabritz-Loutsevitch, N.; Ostrom, R. S.; Slominski, A. T. Melatonin membrane receptors in peripheral tissues: distribution and functions. *Mol Cell Endocrinol* **351:**152-166; 2012.

[7] Esposito, E.; Cuzzocrea, S. Antiinflammatory activity of melatonin in central nervous system. *Curr Neuropharmacol* **8:**228-242; 2010.

[8] Galano, A.; Tan, D. X.; Reiter, R. J. Melatonin as a natural ally against oxidative stress: a physicochemical examination. *J. Pineal Res.* **51:**1–16; 2011.

[9] Pandi-Perumal, S. R.; Kramer, M. "Melatonin and mental illness," in Sleep and Mental Illness. *Cambridge University Press* **UK:**119–129; 2010.

[10] Babaee, A.; Eftekhar-Vaghefi, S. H.; Asadi-Shekaari, M.; Shahrokhi, N.; Soltani, S. D.; Malekpour-Afshar, R.; Basiri, M. Melatonin treatment reduces astrogliosis and apoptosis in rats with traumatic brain injury. *Iran J Basic Med Sci* **18:**867-872; 2015.

[11] Dehghan, F.; Khaksari Hadad, M.; Asadikram, G.; Najafipour, H.; Shahrokhi, N. Effect of melatonin on intracranial pressure and brain edema following traumatic brain injury: role of oxidative stresses. *Arch Med Res* **44:**251-258; 2013.

[12] Tsai, M. C.; Chen, W. J.; Tsai, M. S.; Ching, C. H.; Chuang, J. I. Melatonin attenuates brain contusion-induced oxidative insult, inactivation of signal transducers and activators of transcription 1, and upregulation of suppressor of cytokine signaling-3 in rats. *J Pineal Res* **51:**233-245; 2011.

[13] Lin, C.; Chao, H.; Li, Z.; Xu, X.; Liu, Y.; Hou, L.; Liu, N.; Ji, J. Melatonin attenuates traumatic brain injury-induced inflammation: a possible role for mitophagy. *J Pineal Res* **61:**177-186; 2016.

[14] Hirai, K.; Kita, M.; Ohta, H.; Nishikawa, H.; Fujiwara, Y.; Ohkawa, S.; Miyamoto, M. Ramelteon (TAK-375) accelerates reentrainment of circadian rhythm after a phase advance of the light-dark cycle in rats. *J Biol Rhythms* **20:**27-37; 2005.

[15] Laudon, M.; Frydman-Marom, A. Therapeutic effects of melatonin receptor agonists on sleep and comorbid disorders. *Int J Mol Sci* **15:**15924-15950; 2014.

[16] Cardinali, D. P.; Srinivasan, V.; Brzezinski, A.; Brown, G. M. Melatonin and its analogs in insomnia and depression. *J Pineal Res* **52:**365-375; 2012.

[17] Kast, R. E. Agomelatine or ramelteon as treatment adjuncts in glioblastoma and other M1- or M2-expressing cancers. *Contemp Oncol (Pozn)* **19:**157-162; 2015.

[18] Lauterbach, E. C.; Victoroff, J.; Coburn, K. L.; Shillcutt, S. D.; Doonan, S. M.; Mendez, M. F. Psychopharmacological neuroprotection in neurodegenerative disease: assessing the preclinical data. *J Neuropsychiatry Clin Neurosci* **22:**8-18; 2010.

[19] Lequerica, A.; Jasey, N.; Portelli Tremont, J. N.; Chiaravalloti, N. D. Pilot study on the effect of ramelteon on sleep disturbance after Traumatic brain injury: preliminary evidence from a clinical trial. *Arch Phys Med Rehabil* **96:**1802-1809; 2015.

[20] Xiong, Y.; Mahmood, A.; Chopp, M. Animal models of traumatic brain injury. *Nat Rev Neurosci* **14:**128-142; 2013.

[21] Cheng, T.; Wang, W.; Li, Q.; Han, X.; Xing, J.; Qi, C.; Lan, X.; Wan, J.; Potts, A.; Guan, F.; Wang, J. Cerebroprotection of flavanol (-)-epicatechin after traumatic brain injury via Nrf2-dependent and -independent pathways. *Free Radic Biol Med* **92:**15-28; 2016.

[22] Cheng, T.; Yang, B.; Li, D.; Ma, S.; Tian, Y.; Qu, R.; Zhang, W.; Zhang, Y.; Hu, K.; Guan, F.; Wang, J. Wharton's jelly transplantation improves neurologic function in a rat model of traumatic brain injury. *Cell Mol Neurobiol* **35:**641-649; 2015.

[23] Li, D.; Ma, S.; Guo, D.; Cheng, T.; Li, H.; Tian, Y.; Li, J.; Guan, F.; Yang, B.; Wang, J. Environmental circadian disruption worsens neurologic impairment and inhibits hippocampal neurogenesis in adult rats after traumatic brain injury. *Cell Mol Neurobiol* **36:**1045-1055; 2016.

[24] Miyamoto, M. Effect of ramelteon (TAK-375), a selective MT1/MT2 receptor agonist, on motor performance in mice. *Neurosci Lett* **402:**201-204; 2006.

[25] Han, X.; Zhao, X.; Lan, X.; Li, Q.; Gao, Y.; Liu, X.; Wan, J.; Yang, Z.; Chen, X.; Zang, W.; Guo, A. M.; Falck, J. R.; Koehler, R. C.; Wang, J. 20-HETE synthesis inhibition promotes cerebral protection after intracerebral hemorrhage without inhibiting angiogenesis. *J Cereb Blood Flow Metab***:**271678X18762645; 2018.

[26] Kasahara, T.; Abe, K.; Mekada, K.; Yoshiki, A.; Kato, T. Genetic variation of melatonin productivity in laboratory mice under domestication. *Proc Natl Acad Sci U S A* **107:**6412-6417; 2010.

[27] Vivien-Roels, B.; Malan, A.; Rettori, M. C.; Delagrange, P.; Jeanniot, J. P.; Pevet, P. Daily variations in pineal melatonin concentrations in inbred and outbred mice. *J Biol Rhythms* **13:**403-409; 1998.

[28] Fisher, S. P.; Davidson, K.; Kulla, A.; Sugden, D. Acute sleep-promoting action of the melatonin agonist, ramelteon, in the rat. *J Pineal Res* **45:**125-132; 2008.

[29] Wisor, J. P.; Jiang, P.; Striz, M.; O'Hara, B. F. Effects of ramelteon and triazolam in a mouse genetic model of early morning awakenings. *Brain Res* **1296:**46-55; 2009.

[30] Wang, J.; Liu, X.; Lu, H.; Jiang, C.; Cui, X.; Yu, L.; Fu, X.; Li, Q.; Wang, J. CXCR4(+)CD45(-) BMMNC subpopulation is superior to unfractionated BMMNCs for protection after ischemic stroke in mice. *Brain Behav Immun* **45:**98-108; 2015.

[31] Jiang, C.; Zuo, F.; Wang, Y.; Lu, H.; Yang, Q.; Wang, J. Progesterone changes VEGF and BDNF expression and promotes neurogenesis after ischemic stroke. *Mol Neurobiol* **54:**571-581; 2017.

[32] Wang, J.; Fu, X.; Zhang, D.; Yu, L.; Lu, Z.; Gao, Y.; Liu, X.; Man, J.; Li, S.; Li, N.; Wang, M.; Liu, X.; Chen, X.; Zang, W.; Yang, Q.; Wang, J. Effects of crenolanib, a

nonselective inhibitor of PDGFR, in a mouse model of transient middle cerebral artery occlusion. *Neuroscience* **364:**202-211; 2017.

[33] Wu, H.; Wu, T.; Hua, W.; Dong, X.; Gao, Y.; Zhao, X.; Chen, W.; Cao, W.; Yang, Q.; Qi, J.; Zhou, J.; Wang, J. PGE2 receptor agonist misoprostol protects brain against intracerebral hemorrhage in mice. *Neurobiol Aging* **36:**1439-1450; 2015.

[34] Lan, X.; Han, X.; Li, Q.; Li, Q.; Gao, Y.; Cheng, T.; Wan, J.; Zhu, W.; Wang, J. Pinocembrin protects hemorrhagic brain primarily by inhibiting toll-like receptor 4 and reducing M1 phenotype microglia. *Brain Behav Immun* **61:**326-339; 2017.

[35] Xu, J.; Wang, H.; Ding, K.; Lu, X.; Li, T.; Wang, J.; Wang, C.; Wang, J. Inhibition of cathepsin S produces neuroprotective effects after traumatic brain injury in mice. *Mediators Inflamm* **2013:**187873; 2013.

[36] Wang, W.; Li, H.; Yu, J.; Hong, M.; Zhou, J.; Zhu, L.; Wang, Y.; Luo, M.; Xia, Z.; Yang, Z. J.; Tang, T.; Ren, P.; Huang, X.; Wang, J. Protective effects of Chinese herbal medicine Rhizoma drynariae in rats after traumatic brain injury and identification of active compound. *Mol Neurobiol* **53:**4809-4820; 2016.

[37] Zhu, W.; Gao, Y.; Chang, C. F.; Wan, J. R.; Zhu, S. S.; Wang, J. Mouse models of intracerebral hemorrhage in ventricle, cortex, and hippocampus by injections of autologous blood or collagenase. *PLoS One* **9:**e97423; 2014.

[38] Zhu, W.; Gao, Y.; Wan, J.; Lan, X.; Han, X.; Zhu, S.; Zang, W.; Chen, X.; Ziai, W.; Hanley, D. F.; Russo, S. J.; Jorge, R. E.; Wang, J. Changes in motor function, cognition, and emotion-related behavior after right hemispheric intracerebral hemorrhage in various brain regions of mouse. *Brain Behav Immun* **69:**568-581; 2018.

[39] Can, A.; Dao, D. T.; Terrillion, C. E.; Piantadosi, S. C.; Bhat, S.; Gould, T. D. The tail suspension test. *J Vis Exp***:**e3769; 2012.

[40] Wang, J.; Fu, X.; Jiang, C.; Yu, L.; Wang, M.; Han, W.; Liu, L.; Wang, J. Bone marrow mononuclear cell transplantation promotes therapeutic angiogenesis via upregulation of the VEGF-VEGFR2 signaling pathway in a rat model of vascular dementia. *Behav Brain Res* **265:**171-180; 2014.

[41] Wang, J.; Fu, X.; Yu, L.; Li, N.; Wang, M.; Liu, X.; Zhang, D.; Han, W.; Zhou, C.; Wang, J. Preconditioning with VEGF enhances angiogenic and neuroprotective effects of bone marrow mononuclear cell transplantation in a rat model of chronic cerebral hypoperfusion. *Mol Neurobiol* **53:**6057-6068; 2016.

[42] Li, Q.; Han, X.; Lan, X.; Gao, Y.; Wan, J.; Durham, F.; Cheng, T.; Yang, J.; Wang, Z.; Jiang, C.; Ying, M.; Koehler, R. C.; Stockwell, B. R.; Wang, J. Inhibition of neuronal ferroptosis protects hemorrhagic brain. *JCI Insight* **2:**e90777; 2017.

[43] Li, Q.; Han, X.; Lan, X.; Hong, X.; Li, Q.; Gao, Y.; Luo, T.; Yang, Q.; Koehler, R. C.; Zhai, Y.; Zhou, J.; Wang, J. Inhibition of tPA-induced hemorrhagic transformation involves adenosine A2b receptor activation after cerebral ischemia. *Neurobiol Dis* **108:**173-182; 2017.

[44] Wang, W. Z.; Zhang, H.; Lee, D. H.; Yu, J. T.; Cheng, T.; Hong, M.; Jiang, S. S.; Fan, H.; Huang, X.; Zhou, J. Y.; Wang, J. Using functional and molecular MRI techniques to detect neuroinflammation and neuroprotection after traumatic brain injury. *Brain Behavior and Immunity* **64:**344-353; 2017.

[45] Jiang, C.; Zuo, F.; Wang, Y.; Wan, J.; Yang, Z.; Lu, H.; Chen, W.; Zang, W.; Yang, Q.;

Wang, J. Progesterone exerts neuroprotective effects and improves long-term neurologic outcome after intracerebral hemorrhage in middle-aged mice. *Neurobiol Aging* **42:**13-24; 2016.

[46] Wu, H.; Wu, T.; Xu, X.; Wang, J.; Wang, J. Iron toxicity in mice with collagenase-induced intracerebral hemorrhage. *J Cereb Blood Flow Metab* **31:**1243-1250; 2011.

[47] Han, X.; Lan, X.; Li, Q.; Gao, Y.; Zhu, W.; Cheng, T.; Maruyama, T.; Wang, J. Inhibition of prostaglandin E2 receptor EP3 mitigates thrombin-induced brain injury. *J Cereb Blood Flow Metab* **36:**1059-1074; 2016.

[48] Wu, H.; Wu, T.; Han, X.; Wan, J.; Jiang, C.; Chen, W.; Lu, H.; Yang, Q.; Wang, J. Cerebroprotection by the neuronal PGE2 receptor EP2 after intracerebral hemorrhage in middle-aged mice. *J Cereb Blood Flow Metab* **37:**39-51; 2017.

[49] Pan, L. N.; Zhu, W.; Li, Y.; Xu, X. L.; Guo, L. J.; Lu, Q.; Wang, J. Astrocytic Toll-like receptor 3 is associated with ischemic preconditioning-induced protection against brain ischemia in rodents. *PLoS One* **9:**e99526; 2014.

[50] Wang, J.; Doré, S. Heme oxygenase-1 exacerbates early brain injury after intracerebral haemorrhage. *Brain* **130:**1643-1652; 2007.

[51] Wu, H.; Wu, T.; Li, M.; Wang, J. Efficacy of the lipid-soluble iron chelator 2,2'-dipyridyl against hemorrhagic brain injury. *Neurobiol. Dis.* **45:**388-394; 2012.

[52] Wang, J.; Fields, J.; Zhao, C.; Langer, J.; Thimmulappa, R. K.; Kensler, T. W.; Yamamoto, M.; Biswal, S.; Dore, S. Role of Nrf2 in protection against intracerebral hemorrhage injury in mice. *Free Radic Biol Med* **43:**408-414; 2007.

[53] Kragel, P. A.; Kano, M.; Van Oudenhove, L.; Ly, H. G.; Dupont, P.; Rubio, A.; Delon-Martin, C.; Bonaz, B. L.; Manuck, S. B.; Gianaros, P. J.; Ceko, M.; Reynolds Losin, E. A.; Woo, C. W.; Nichols, T. E.; Wager, T. D. Generalizable representations of pain, cognitive control, and negative emotion in medial frontal cortex. *Nat Neurosci* **21:**283-289; 2018.

[54] Simon, D. W.; McGeachy, M. J.; Bayir, H.; Clark, R. S.; Loane, D. J.; Kochanek, P. M. The far-reaching scope of neuroinflammation after traumatic brain injury. *Nat Rev Neurol* **13:**171-191; 2017.

[55] Ding, K.; Wang, H.; Xu, J.; Lu, X.; Zhang, L.; Zhu, L. Melatonin reduced microglial activation and alleviated neuroinflammation induced neuron degeneration in experimental traumatic brain injury: Possible involvement of mTOR pathway. *Neurochem Int* **76:**23-31; 2014.

[56] Shimizu, N.; Nozawa, M.; Sugimoto, K.; Yamamoto, Y.; Minami, T.; Hayashi, T.; Yoshimura, K.; Ishii, T.; Uemura, H. Therapeutic efficacy and anti-inflammatory effect of ramelteon in patients with insomnia associated with lower urinary tract symptoms. *Res Rep Urol* **5:**113-119; 2013.

[57] Bano Otalora, B.; Popovic, N.; Gambini, J.; Popovic, M.; Vina, J.; Bonet-Costa, V.; Reiter, R. J.; Camello, P. J.; Rol, M. A.; Madrid, J. A. Circadian system functionality, hippocampal oxidative stress, and spatial memory in the APPswe/PS1dE9 transgenic model of Alzheimer disease: effects of melatonin or ramelteon. *Chronobiol Int* **29:**822-834; 2012.

[58] Lan, X.; Han, X.; Li, Q.; Wang, J. (-)-Epicatechin, a Natural Flavonoid Compound,

Protects Astrocytes Against Hemoglobin Toxicity via Nrf2 and AP-1 Signaling Pathways. *Mol Neurobiol* **54:**7898-7907; 2017.

[59] Zhang, L.; Wang, H. Targeting the NF-E2-Related Factor 2 Pathway: a Novel Strategy for Traumatic Brain Injury. *Mol Neurobiol* **55:**1773-1785; 2018.

[60] Ding, K.; Wang, H.; Xu, J.; Li, T.; Zhang, L.; Ding, Y.; Zhu, L.; He, J.; Zhou, M. Melatonin stimulates antioxidant enzymes and reduces oxidative stress in experimental traumatic brain injury: the Nrf2-ARE signaling pathway as a potential mechanism. *Free Radic Biol Med* **73:**1-11; 2014.

[61] Sayeed, M. S. B.; Alhadidi, Q.; Shah, Z. A. Cofilin signaling in hemin-induced microglial activation and inflammation. *J Neuroimmunol* **313:**46-55; 2017.

[62] Jin, W.; Zhu, L.; Guan, Q.; Chen, G.; Wang, Q. F.; Yin, H. X.; Hang, C. H.; Shi, J. X.; Wang, H. D. Influence of Nrf2 genotype on pulmonary NF-kappaB activity and inflammatory response after traumatic brain injury. *Ann Clin Lab Sci* **38:**221-227; 2008.

[63] Yang, Y.; Wang, H.; Li, L.; Li, X.; Wang, Q.; Ding, H.; Wang, X.; Ye, Z.; Wu, L.; Zhang, X.; Zhou, M.; Pan, H. Sinomenine Provides Neuroprotection in Model of Traumatic Brain Injury via the Nrf2-ARE Pathway. *Front Neurosci* **10:**580; 2016.

[64] Li, B. X.; Dong, W. W.; Cheng, H.; Sun, Y. F.; Wang, S.; Chen, J. W.; Jiang, Z. F.; Fu, J. Q.; Pi, J. B.; Guan, D. W.; Zhao, R. Ablation of Nrf2 exacerbated the activation and proliferation of astrocytes in ipsilateral cortex and hippocampus after Traumatic brain injury in mice *The 12th biennial conference of Chinese neuroscience society***:**755-756; 2017.

[65] Wu, G.; Liu, Z. Nuclear Factor Erythroid 2-Related Factor 2 (Nrf2) Mediates

Neuroprotection in Traumatic Brain Injury at Least in Part by Inactivating Microglia. *Med Sci Monit* **22:**2161-2166; 2016.

[66] Yan, W.; Wang, H. D.; Hu, Z. G.; Wang, Q. F.; Yin, H. X. Activation of Nrf2-ARE pathway in brain after traumatic brain injury. *Neurosci Lett* **431:**150-154; 2008.

[67] Dong, W. W.; Li, B. X.; Sun, Y. F.; Guan, D. W.; Zhao, R. Dynamic and cell-type specific Expression of Nrf2 after Traumatic Brain Injury in mice *The 12th Bbiennial Conference of Chinese Neuroscience Society***:**754-755; 2017.

[68] Greenblatt, D. J.; Harmatz, J. S.; Karim, A. Age and gender effects on the pharmacokinetics and pharmacodynamics of ramelteon, a hypnotic agent acting via melatonin receptors MT1 and MT2. *J Clin Pharmacol* **47:**485-496; 2007.

Figure legends

Fig. 1. Ramelteon reduces brain lesion volume and edema and mitigates neurologic deficits and depression-like behaviors after TBI. (**A**) Cresyl violet-stained brain sections at 3 and 28 days post-TBI. Injured areas lack staining and are circled in black (Scale bar = 1 mm). (**B**) Ramelteon decreased lesion volumes at 3 and 28 days post-TBI. n = 8 mice/group.*P<0.05 vs. vehicle group (t-test). (**C**) At 3 days post-TBI, ramelteon reduced brain water content of the ipsilateral hemisphere, but not cerebellum. n = 10 mice/group. *P<0.05 vs. vehicle group (one-way ANOVA followed by Bonferroni post hoc test). (**D**) Mice treated with ramelteon gained body weight more quickly than did mice treated with vehicle and weighed significantly more on day 7 after TBI. n = 10 mice/group. *P<0.05 vs. sham group; $^{\#}P$ < 0.05 vs. vehicle group (repeated measures ANOVA followed by Bonferroni post hoc test). (**E**) Ramelteon failed to enhance the survival rate during the first week after TBI. n = 10 mice/group. **(F)** Neurologic deficit scores were lower in ramelteon-treated mice than in vehicle-treated mice at all time points except for day 1 after TBI. n = 10 mice/group. *P<0.05 vs. sham group; $^{\#}P$< 0.05 vs. vehicle group (repeated measures ANOVA followed by Bonferroni post hoc test). (**G**, **H**) Ramelteon-treated mice exhibited less immobility time in the forced swim test (FST) and tail suspension test (TST) on day 28. n = 10 mice/group. *P<0.05 vs. sham group; $^{\#}P$< 0.05 vs. vehicle group (one-way ANOVA). (**I**) Ramelteon-treated mice consumed more sucrose-sweetened water than did vehicle-treated mice in the sucrose preference test (SPT). n = 10 mice/group. *P<0.05 vs. sham group; $^{\#}P$< 0.05 vs. vehicle group (one-way ANOVA followed by Bonferroni post hoc test). Data are expressed as mean ± SD.

Fig. 2. Ramelteon improves learning and memory functions in mice after TBI. (**A**) Typical escape route across the training days (upper) and the trajectories of mice during the probe trial period (lower) of the Morris water maze (MWM) test. (**B**) In the MWM test, ramelteon decreased escape latency on the last two training days. n = 10 mice/group. **P*<0.05 vs. sham group; $^{\#}P$<0.05 vs. vehicle group (repeated measures ANOVA followed by Bonferroni post hoc test). (**C**, **D**) Ramelteon did not affect the average swimming speed during the training days (**C**) or during the probe trial period on day 28 (**D**). (**E**, **F**) During the probe trial on day 28, ramelteon-treated mice spent significantly more time in the target quadrant (**E**) than did the vehicle-treated mice and crossed the platform location more times (**F**). n = 10 mice/group. **P*<0.05 vs. sham group; $^{\#}P$<0.05 vs. vehicle group (one-way ANOVA followed by Bonferroni post hoc test). (**G**) Ramelteon increased the discrimination index in the novel object recognition test. n = 10 mice/group. **P*<0.05 vs. sham group; $^{\#}P$<0.05 vs. vehicle group (one-way ANOVA followed by Bonferroni post hoc test). Data are expressed as mean ± SD.

Fig. 3. Ramelteon attenuates the inflammatory response and oxidative stress in brain tissue and serum of mice after TBI. (**A**) Ramelteon increased anti-inflammatory cytokines IL-10 and IL-4 but decreased pro-inflammatory cytokines IL-1β and TNF-α in brain tissue and serum on days 1, 3, and 7 after TBI. n = 6 mice/group. **P*<0.05 vs. sham group; $^{\#}P$<0.05 vs. vehicle group (one-way ANOVA followed by Bonferroni post hoc test). (**B**) Ramelteon markedly increased the levels of superoxide dismutase (SOD), glutathione (GSH), and

glutathione peroxidase (GSH-Px) and decreased the level of malondialdehyde (MDA) in brain tissue and serum on days 1, 3, and 7 after TBI. n = 6 mice/group. *P<0.05 vs. sham group; $^{\#}P$<0.05 vs. vehicle group (one-way ANOVA followed by Bonferroni post hoc test). (**C**, **D**) Representative images of immunofluorescence staining for GFAP (**C**) and Iba-1 (**D**) in the perilesional region of the injured frontal cortex on day 3 (Scale bar = 50 μm). Ramelteon decreased the number of activated microglia and astrocytes (in red) after TBI. Insets show merged images of GFAP or IBA-1 staining with DAPI-stained nuclei. n=6 mice/group.*P<0.05 vs. sham group; $^{\#}P$<0.05 vs. vehicle group (one-way ANOVA followed by Bonferroni post hoc test). Data are expressed as mean ± SD. Iba1, ionized calcium-binding adapter molecule 1, GFAP, glial fibrillary acidic protein.

Fig. 4. Ramelteon decreases Keap1 expression, promotes nuclear accumulation of Nrf2, and increases the expression of Nrf2 downstream molecules after TBI. (**A-C**) Western blotting showed that ramelteon decreased Keap1 expression (**A**) and increased nuclear Nrf2 expression (**B**), but did not affect cytoplasmic Nrf2 expression (**C**). n = 5 mice/group. *P< 0.05 vs. sham group; $^{\#}P$ < 0.05 vs. vehicle group (one-way ANOVA followed by Bonferroni post hoc test). (**D-F**) Western blotting showed that ramelteon increased the expression of cytoplasmic proteins superoxide dismutase-1 (SOD1; **D**), hemoxygenase-1 (HO-1; **E**), and NQO1 (**F**) on day 3 post-TBI. n = 5 mice/group. *P<0.05 vs. sham group; $^{\#}P$<0.05 vs. vehicle group (one-way ANOVA followed by Bonferroni post hoc test). Data are expressed as mean ± SD.

Fig. 5. The neuroprotection conferred by ramelteon is mostly lost in Nrf2 KO mice after TBI. (**A**) Cresyl violet and Luxol fast blue staining on day 3 post-TBI. Injured areas lack staining and are outlined in black (Scale bar: 1 mm). (**B**, **C**) Ramelteon failed to decrease lesion volume on day 3 (**B**) or mortality during the first week (**C**) in Nrf2 KO mice. n = 10 mice/group. (**D**) Ramelteon-treated Nrf2 KO mice exhibited a greater increase in body weight than did vehicle-treated Nrf2 KO mice on day 3. n = 10 mice/group. **P*<0.05 vs. vehicle group (repeated measures ANOVA followed by Bonferroni post hoc test). (**E**) Neurologic deficits were less severe in ramelteon-treated Nrf2 KO mice than in vehicle-treated Nrf2 KO mice on days 14 and 28 post-TBI. n = 10 mice/group. **P*<0.05 vs. sham group (repeated measures ANOVA followed by Bonferroni post hoc test). Ramelteon did not improve motor performance of Nrf2 KO mice in the wire-hanging test (**F**), rotarod test (**G**), or left paw placement test (**H**) on days 7, 14, and 28 after TBI. n = 10 mice/group. Similarly, ramelteon did not alleviate memory deficits of Nrf2 KO mice in the novel object recognition test (**I**) or depression-like behaviors in the tail suspension test (TST; **J**), forced swim test (FST; **K**), or sucrose preference test (**L**) on day 28 after TBI. n = 10 mice/group. **P*<0.05 vs. sham group (one-way ANOVA followed by Bonferroni post hoc test). (**M**) (Left) Cresyl violet and Luxol fast blue staining of ipsilateral corpus striatum on day 3 post-TBI. Scale bar = 50 μm. (Right) Bar graph shows that ramelteon did not increase the percentage of area with normal myelin in the Nrf2 KO mouse brain compared with that in the vehicle group. n = 6 mice/group. **P*<0.05 vs. sham group (one-way ANOVA followed by Bonferroni post hoc test). **(N)** (Left) Fluoro-Jade C staining of the perilesional cerebral cortex on day 3 post-TBI. Scale bar = 30 μm. (Right) Bar graph shows that ramelteon did not decrease the number of degenerating

neurons in the perilesional region of the Nrf2 KO mice. n = 6 mice/group. *P<0.05 vs. sham group (one-way ANOVA followed by Bonferroni post hoc test).

Highlights

1. Ramelteon provided marked neuroprotection after TBI.
2. Ramelteon activated the Nrf2-ARE pathway in the brain after TBI.
3. The protection by ramelteon was partially lost in Nrf2$^{-/-}$ mice with TBI.

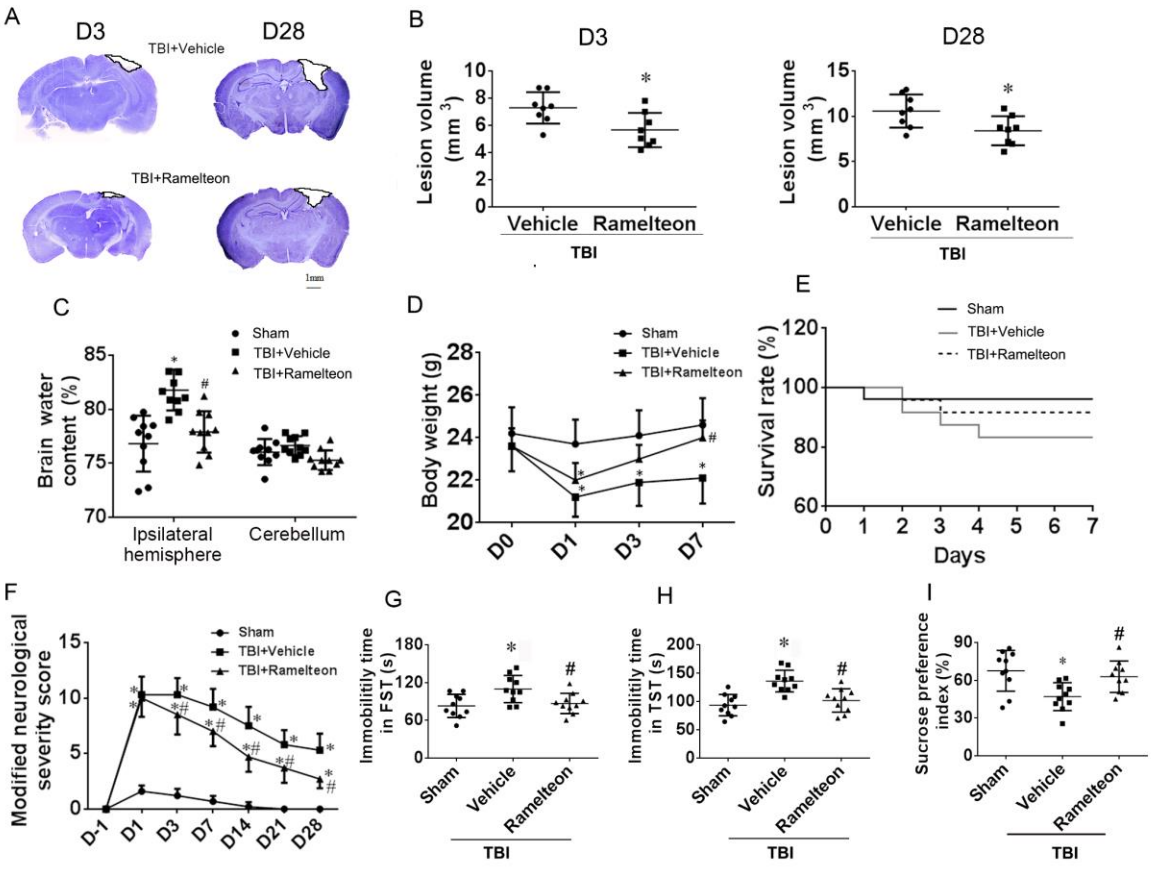

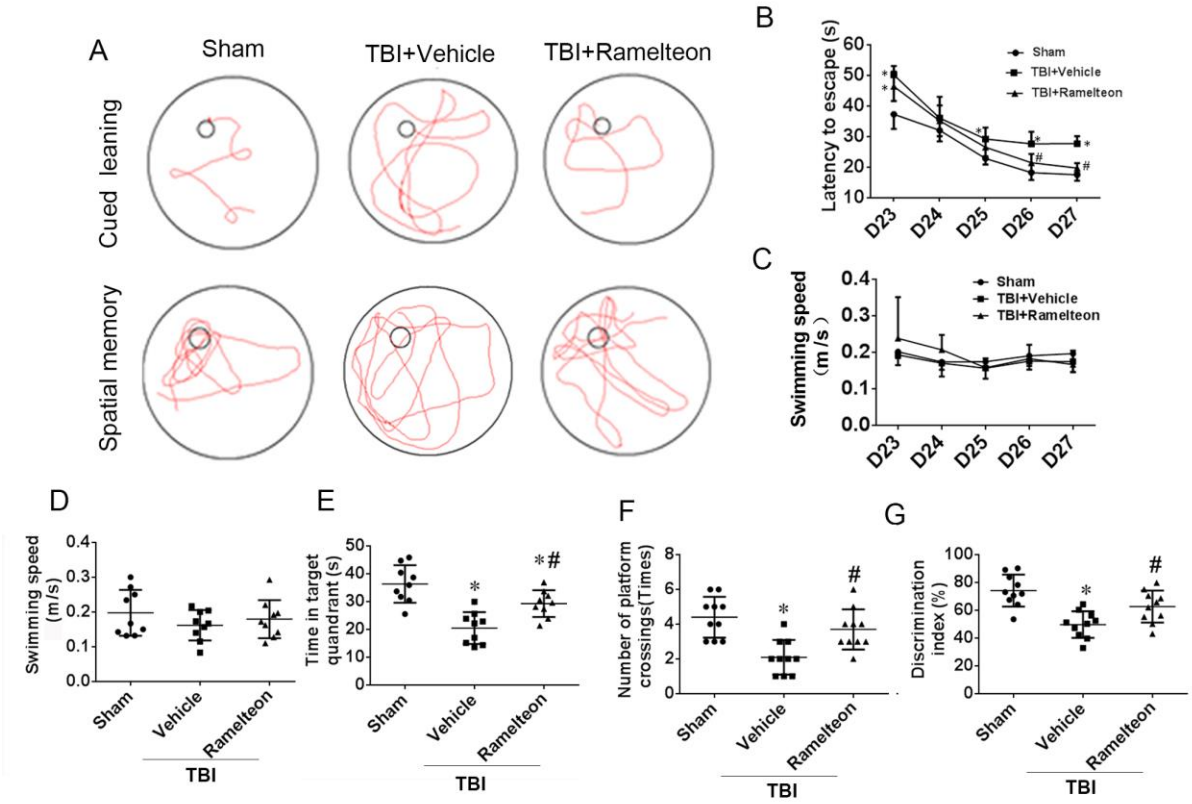
A
Sham
TBI+Vehicle
TBI+Ramelteon
Cued leaning
Spatial memory
B
Latency to escape (s)
Sham
TBI+Vehicle
TBI+Ramelteon
D23
D24
D25
D26
D27
C
Swimming speed (m/s)
D
Swimming speed (m/s)
E
Time in target quandrant (s)
F
Number of platform crossings(Times)
G
Discrimination index (%)
Sham
Vehicle
Ramelteon
TBI

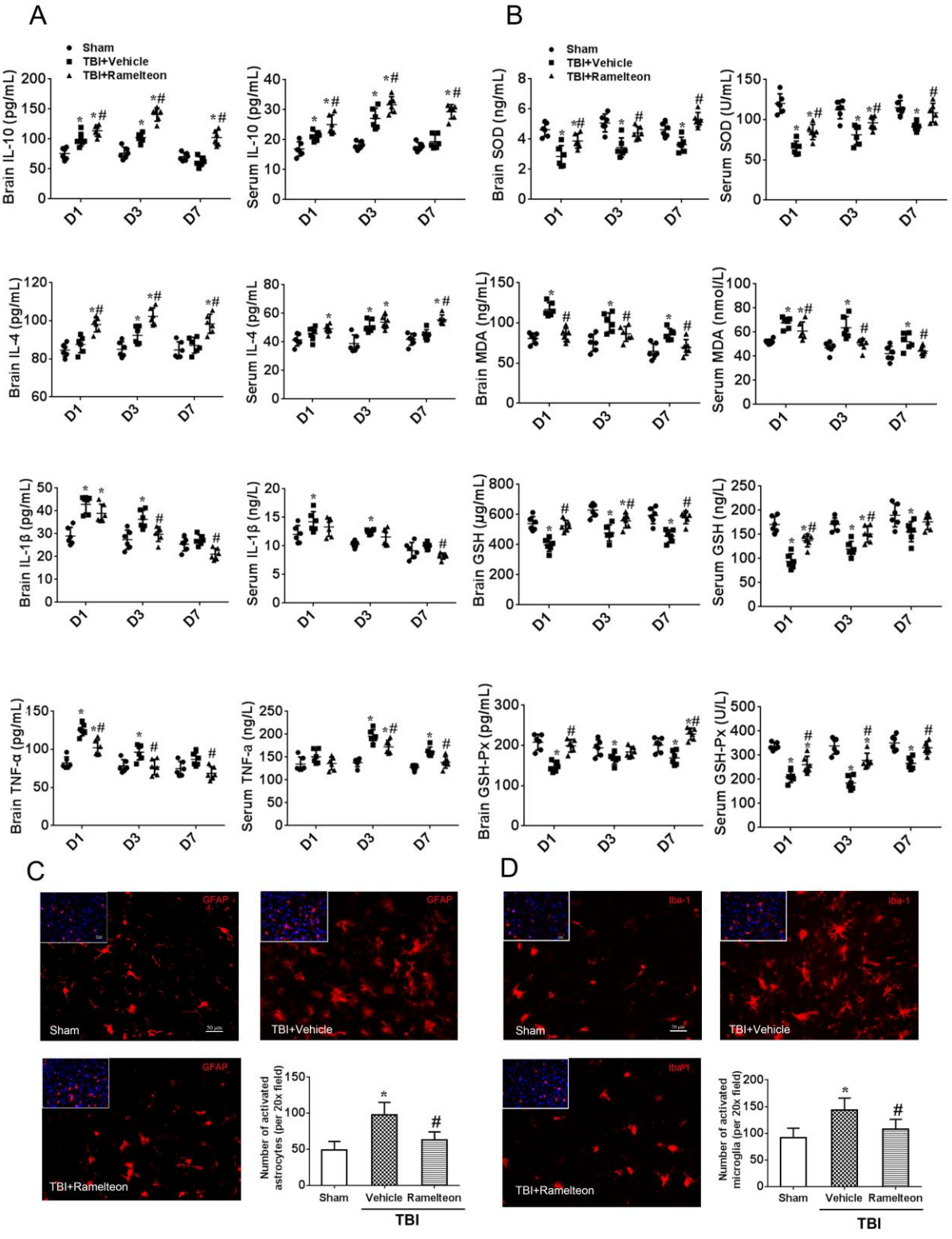
A
B
Sham
TBI+Vehicle
TBI+Ramelteon
Brain IL-10 (pg/mL)
Serum IL-10 (pg/mL)
Brain SOD (ng/mL)
Serum SOD (U/mL)
Brain IL-4 (pg/mL)
Serum IL-4 (pg/mL)
Brain MDA (ng/mL)
Serum MDA (nmol/L)
Brain IL-1β (pg/mL)
Serum IL-1β (ng/L)
Brain GSH (μg/mL)
Serum GSH (ng/L)
Brain TNF-α (pg/mL)
Serum TNF-a (ng/L)
Brain GSH-Px (pg/mL)
Serum GSH-Px (U/L)
D1
D3
D7
C
D
GFAP
Iba-1
Sham
TBI+Vehicle
TBI+Ramelteon
Number of activated astrocytes (per 20x field)
Number of activated microglia (per 20x field)
Vehicle
Ramelteon
TBI

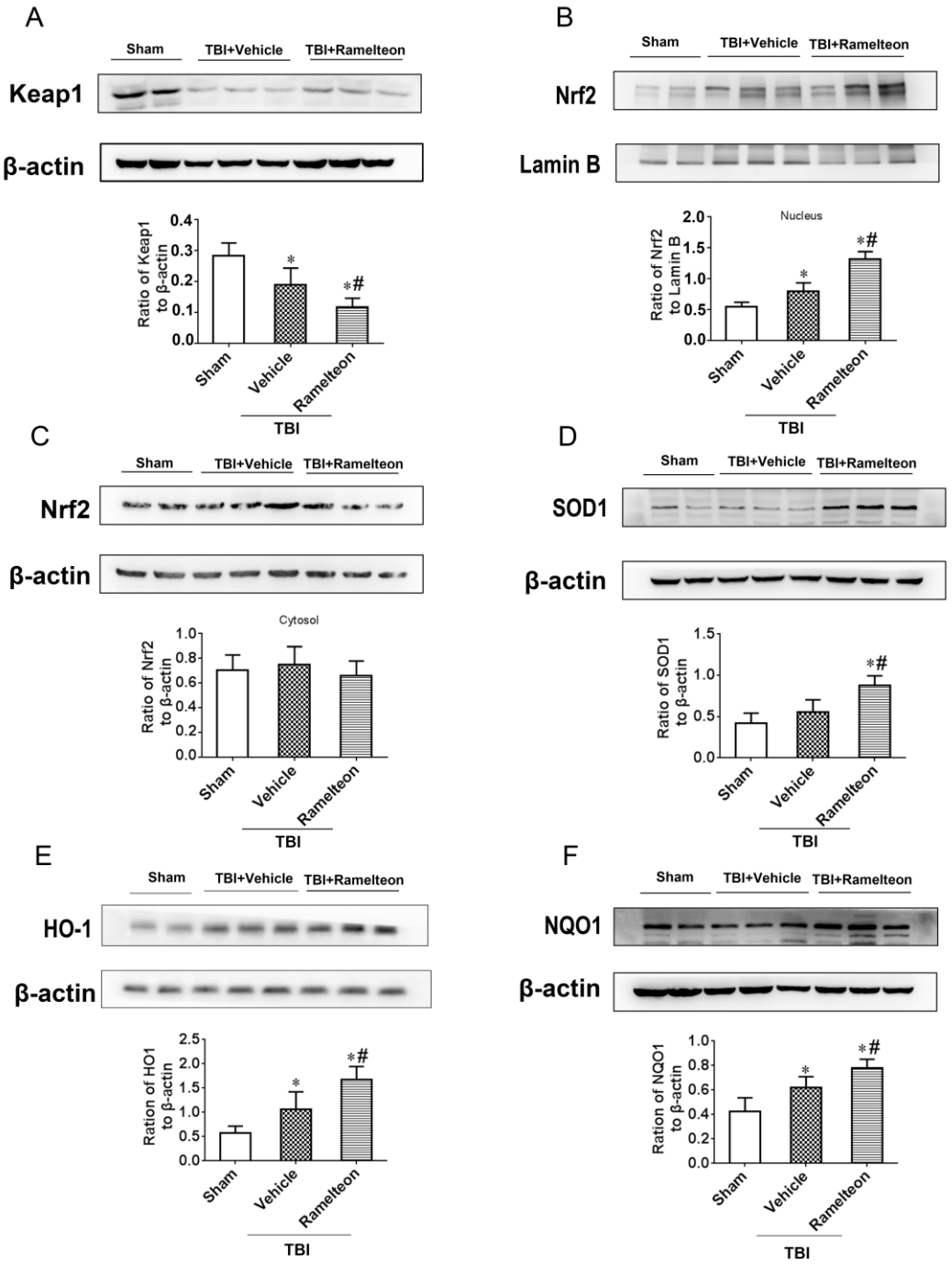
A
Sham
TBI+Vehicle
TBI+Ramelteon
Keap1
β-actin
Ratio of Keap1 to β-actin
0.4
0.3
0.2
0.1
0.0
*
*#
Sham
Vehicle
Ramelteon
TBI
B
Sham
TBI+Vehicle
TBI+Ramelteon
Nrf2
Lamin B
Nucleus
Ratio of Nrf2 to Lamin B
2.0
1.5
1.0
0.5
0.0
*
*#
Sham
Vehicle
Ramelteon
TBI
C
Sham
TBI+Vehicle
TBI+Ramelteon
Nrf2
β-actin
Cytosol
Ratio of Nrf2 to β-actin
1.0
0.8
0.6
0.4
0.2
0.0
Sham
Vehicle
Ramelteon
TBI
D
Sham
TBI+Vehicle
TBI+Ramelteon
SOD1
β-actin
Ratio of SOD1 to β-actin
1.5
1.0
0.5
0.0
*#
Sham
Vehicle
Ramelteon
TBI
E
Sham
TBI+Vehicle
TBI+Ramelteon
HO-1
β-actin
Ration of HO1 to β-actin
2.5
2.0
1.5
1.0
0.5
0.0
*
*#
Sham
Vehicle
Ramelteon
TBI
F
Sham
TBI+Vehicle
TBI+Ramelteon
NQO1
β-actin
Ration of NQO1 to β-actin
1.0
0.8
0.6
0.4
0.2
0.0
*
*#
Sham
Vehicle
Ramelteon
TBI

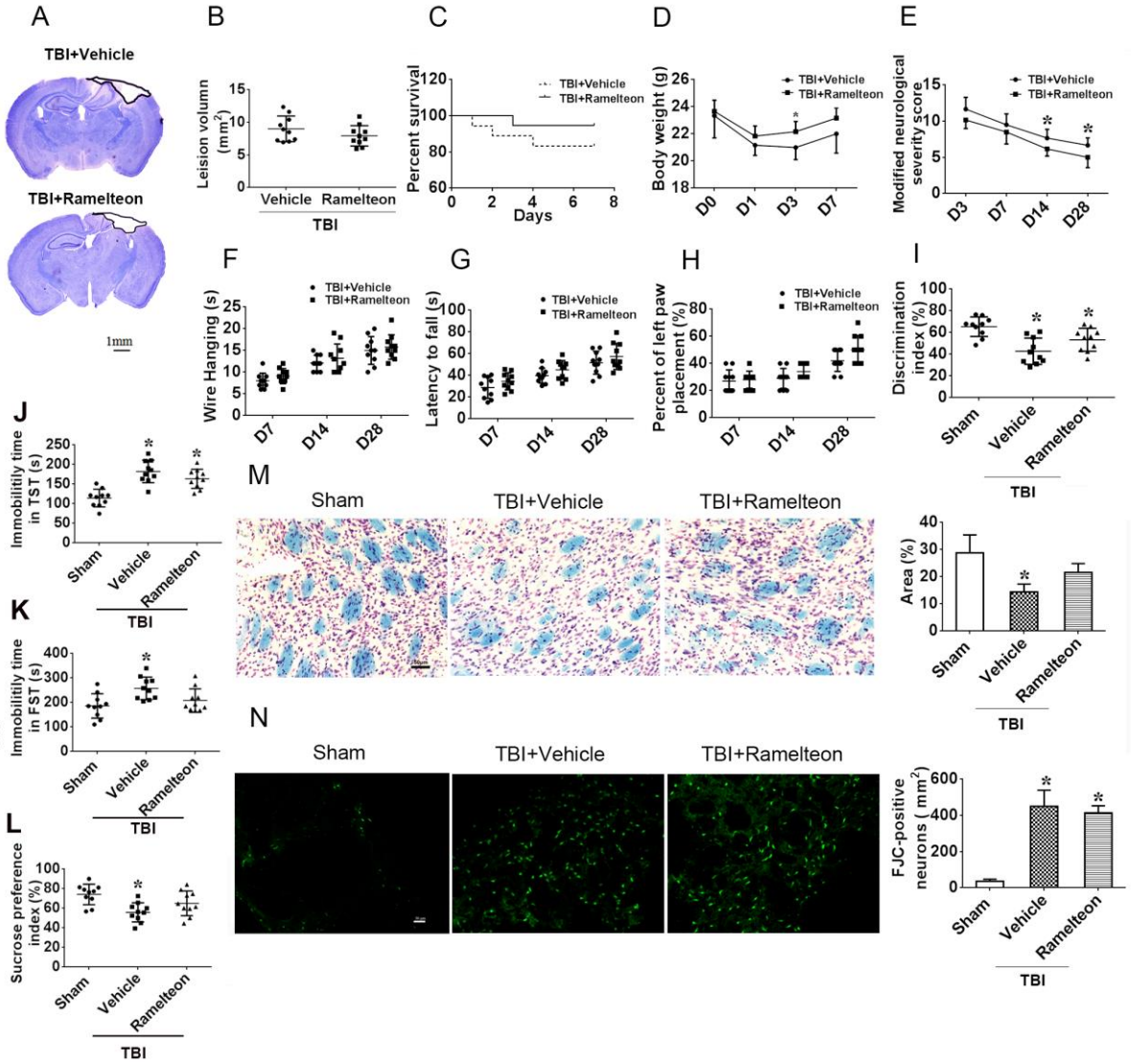
A
TBI+Vehicle
TBI+Ramelteon
1mm
B
Leision volumn (mm²)
Vehicle
Ramelteon
TBI
C
Percent survival
TBI+Vehicle
TBI+Ramelteon
Days
D
Body weight (g)
TBI+Vehicle
TBI+Ramelteon
D0
D1
D3
D7
E
Modified neurological severity score
TBI+Vehicle
TBI+Ramelteon
D3
D7
D14
D28
F
Wire Hanging (s)
TBI+Vehicle
TBI+Ramelteon
D7
D14
D28
G
Latency to fall (s)
TBI+Vehicle
TBI+Ramelteon
D7
D14
D28
H
Percent of left paw placement (%)
TBI+Vehicle
TBI+Ramelteon
D7
D14
D28
I
Discrimination index (%)
Sham
Vehicle
Ramelteon
TBI
J
Immobilitily time in TST (s)
Sham
Vehicle
Ramelteon
TBI
K
Immobilitily time in FST (s)
Sham
Vehicle
Ramelteon
TBI
L
Sucrose preference index (%)
Sham
Vehicle
Ramelteon
TBI
M
Sham
TBI+Vehicle
TBI+Ramelteon
Area (%)
Sham
Vehicle
Ramelteon
TBI
N
Sham
TBI+Vehicle
TBI+Ramelteon
FJC-positive neurons (mm²)
Sham
Vehicle
Ramelteon
TBI